

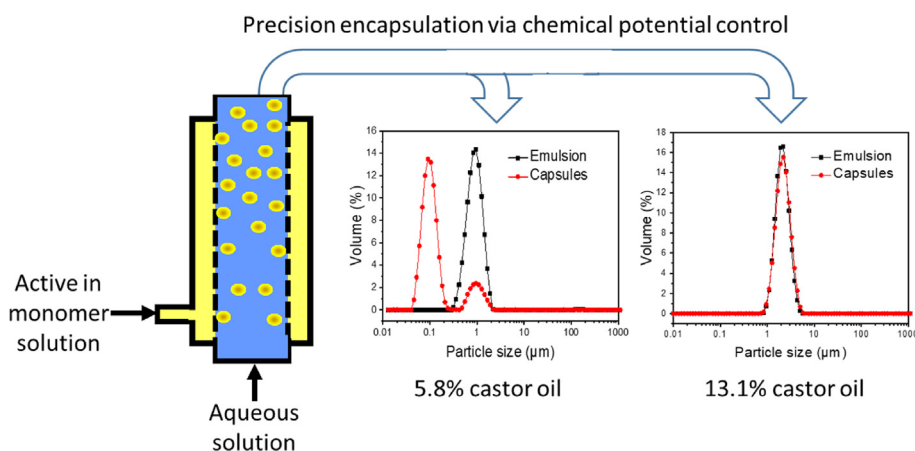
Critical role of chemical potential to assure effective encapsulation

Qingchun Yuan^{1,*}, Stephen Collins, Joyleen Poole, Xiaodong Jia, Richard A. Williams²

School of Chemical and Process Engineering, University of Leeds, Leeds LS2 9JT, UK



GRAPHICAL ABSTRACT



ARTICLE INFO

Article history:

Received 20 March 2022

Revised 30 April 2022

Accepted 3 May 2022

Available online 6 May 2022

Keywords:

Chemical potential

Polymerisation-encapsulation

Castor oil

Hydrophobe

Membrane emulsification

ABSTRACT

Hypothesis: In emulsification-polymerisation avoiding monomer escape from emulsion droplets is the key to successful encapsulation. So far, it is believed that (1) a hydrophobe needs to be included and (2) free-micelles of surfactant need to be depleted. However, these criteria do not always work. The paper explores the critical role of the chemical potential difference between the inside and outside of the emulsion droplet for successful encapsulation.

Experiments: Crossflow membrane emulsification was used to produce uniform droplets of 1–2 μm of solutions of 3-iodoprop-2-yn-1-yl butylcarbamate (a biocide), castor oil (hydrophobe) in methyl 2-methylprop-2-enoate (monomer) into aqueous solutions with a large amount of free-micelles of surfactant. The encapsulation was followed by polymerisation. The size distribution of microcapsule from different formula were examined.

Findings: The biocide encapsulation depends on castor oil content: >12% (full); 6–12% (either full or partial); <6% (minor). Results show a critical molar fraction ratio of the monomer in the droplet to water in the aqueous phase that provides a definitive criterion to assure size retention and full encapsulation. This critical value corresponds to an energy barrier of 116 J/mol to prevent the monomer escaping. This finding is proposed to be used as an advanced rule to guide precision formulation for desired microencapsulation.

© 2022 Published by Elsevier Inc.

* Corresponding author.

E-mail address: q.yuan@aston.ac.uk (Q. Yuan).

¹ Present address: College of Engineering and Physical Sciences, Aston University, Birmingham B4 7ET, UK.

² Present address: Heriot-Watt University, Edinburgh EH14 4AS, UK.

1. Introduction

Microcapsules are advanced delivery vehicles for precious functional active components such as fragrances [1], flavours [1], vitamins [2], cosmetic products [3], insecticide [4] and cancer drugs [5]. It is a common requirement to precisely control both particle size/size distribution and capsule structure to achieve desired release profiles, overall appearance and performance. A two-step process of emulsification and encapsulation is frequently chosen to achieve a controlled production [6]. Such a process disperses a phase containing the active component (the ‘disperse phase’) into an immiscible one (the ‘continuous phase’) in the emulsification step before carrying out a subsequent encapsulation step. Polymers are widely used as encapsulating materials, since they offer a range of chain structures and conformation, compatible to the active component and the end use environment.

There is much interest in the use of methyl 2-methylprop-2-enoate (MMA) and styrene to form microcapsules. To ensure active components in the monomer droplets are well encapsulated, it is essential that the monomer polymerises only within the droplet (i.e. suspension polymerisation). Ideally, the polymer polymerised forms a continuous shell between the active and the continuous phase as individual spherical particles. The microcapsules so formed will ideally replicate the size and size distribution of their emulsion precursors with the active component inside. However, this is not often the case.

MMA and styrene monomers have a significant solubility in water, 1.6 g/100 ml water for MMA and 0.3 g/100 ml water for styrene at 20 °C. The monomer diffusion from the dispersed droplet to the aqueous continuous phase will result in a significant amount of monomer escaping from the droplet to the continuous phase [7]. When the polymerisation is occurring, escaping monomer molecules in the aqueous phase will polymerise in the free micelles of surfactant in the continuous phase and gradually deplete the monomer molecules. The depletion will drive the process of the monomer in the droplet diffusing continuously to the continuous phase and lead to the formation of secondary nucleated polymer particles without the active being encapsulated. Such a mechanism is called emulsion polymerisation, where the monomer droplets play a role of reservoir to provide monomer gradually and water-soluble initiators facilitate this process.

The following strategies have been developed to steer polymerisation away from emulsion polymerisation and so to follow suspension mechanism [8–14]:

- Limiting the monomer escape by generating an osmotic pressure inside the droplet to balance the Laplace pressure caused by the droplet curvature [8]. The osmotic pressure can be generated by adding a hydrophobic agent in the disperse phase, which needs to have a very low solubility in water.
- Limiting the existence of free micelles of surfactant in the continuous phase by using a concentration lower than the critical micelle concentration (CMC) of the surfactant.
- Using non-water-soluble initiators.

Landfester et al. [8] suggested that an effective hydrophobic agent needs to have a solubility in water less than 10^{-7} mL mL⁻¹, and a molar ratio of an effective hydrophobe to the monomer above 1:250 to establish the osmotic pressure required to overcome the action of Laplace pressure for monomer droplets in the range of 50–150 nm to be stabilised during polymerisation. Hexadecane has been used as an effective osmotic agent in monomer droplets for its very low solubility in water (6.3×10^{-7} g in 100 g water at 25 °C). By including ~4 wt% of hexadecane in styrene or MMA monomer phase and controlling the surfactant

(sodium dodecylsulphate, SDS) concentration in a regime lower than its CMC but still being able to provide satisfied stabilisation of monomer nano-droplet in the aqueous solution Landfester et al. [8,9] prepared stable miniemulsions and achieved so-called 1:1 copied polymer particles (suspension polymerisation of nano-emulsion). The concentration regime varies with droplet sizes, and Oswald ripening can occur resulting in larger emulsion droplets if the monomer droplets are not well covered by surfactant molecules. Controlling the surfactant concentration is therefore critical for polymer particle size and size distribution control.

Ma and Li [10] carefully prepared mono-dispersed styrene monomer emulsions (in the range of 8–24 μm) by membrane emulsification for their study of polymerisation. Two polymerisation mechanisms were identified—polymerisation in micro-sized monomer droplets and nano-sized secondary nuclei, even in the presence of a hydrophobic initiator and a hydrophobic additive (hexadecane). Increasing the amount of a hydrophobic additive (10–50 wt% of hexadecane), and/or adding a water-soluble inhibitor in the aqueous phase suppressed the polymerisation in the secondary nuclei. They used 10–50 wt% of hexadecane in the styrene monomer phase, SDS concentration in the aqueous phase at 1.2 mM well below its CMC (8.27 mM at 25 °C), and included salt (Na₂SO₄) and PVP (1-ethenylpyrrolidin-2-one) in the aqueous phase to co-stabilise the monomer droplet. They encountered the monomer escaping from its droplet and the formation of smaller polymer particles (~0.2 μm). Under the condition where a hydrophilic monomer was added, hollow microspheres were formed when polymerisation in the secondary nuclei was dominant, while one-hole microspheres resulted when polymerisation occurred only inside the larger monomer droplets, indicating that the compromise between dominant mechanisms is critical to the polymerisation process. This observation is in conflict with Landfester’s results that the increase in polymer particle sizes is due to collision of poorly covered monomer droplets [8].

Landfester et al. [8] believed that the bare presence of a hydrophobe (4 wt% [15]) rather than the absolute osmotic pressure influences the particle size. However, Ma and Li’s work clearly demonstrated that the bare presence of hydrophobe (5–10 wt%) could not suppress the escape of monomers, and increasing the amount of hydrophobe did reduce the polymerisation outside the monomer droplet [10], but the incompletely covered interface could not completely prevent the monomer escaping. Comparing Ma and Li’s results to that of Landfester et al. [8], droplets in the size range of micrometres should be more capable of preventing monomer escape than that in nanometres, for the later gives rise to larger Laplace pressures. The effect of hydrophobe, surfactant concentration and type of initiator on polymerisation mechanisms is not fully understood yet.

Along with hexadecane, many other components, e.g. olive oil [8], tetraethylsilane [8], hydrocarbon coumarone-indene resin [15], Miglyol 812 [16], and (briefly) castor oil [16,17] have been used as a hydrophobe.

Membrane emulsification is a technique that produces emulsion droplets through extrusion of one liquid phase through micropores in a membrane into a second liquid phase [6,18]. The use of membranes to manufacture emulsions and other soft and hard particulates such as microcapsules can achieve a high degree of size control and consistency. In crossflow membrane emulsification (XME) the continuous phase is forced to flow across the membrane surface as shown in Fig. 1. A pressure is applied to the disperse phase which forces it to permeate the membrane pores and form disperse phase droplets on the inner surface of the membrane in the path of the flowing continuous phase. The shear force caused by the cross flowing assists in the detachment of the droplets formed into the continuous phase.

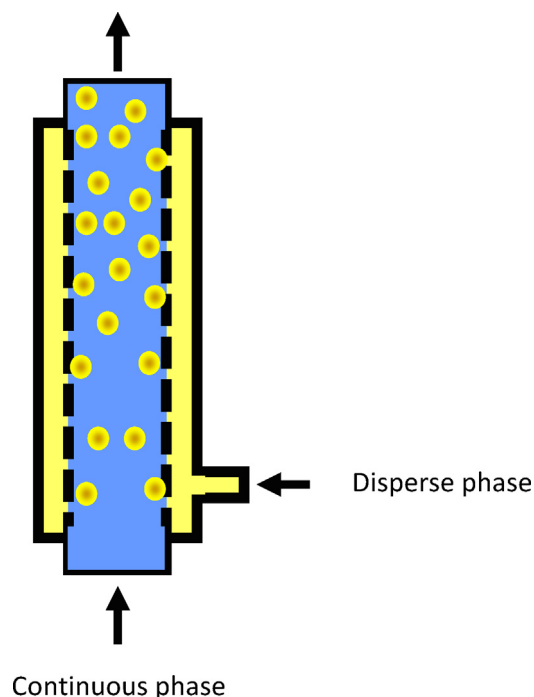


Fig. 1. Schematic diagram of XME.

In this work we report the successful 1:1 copied suspension polymerisation for complete encapsulation of a biocide, 3-iodoprop-2-yn-1-yl butylcarbamate (IPBC), in polymer microcapsules size-ranged around 1–2 μm through membrane emulsification and suspension polymerisation. The monomer phase of methyl 2-methylprop-2-enoate (MMA) containing an active ingredient (IPBC, 5.9–15.9 wt%) and castor oil (3.1–23.5 wt%) as hydrophobic agent was emulsified into a simple aqueous solution of SDS at 31.0 mM, which is well above its CMC (8.2 mM in pure water at 25 °C). The effect of hydrophobe (castor oil) concentration on the emulsification and encapsulation behaviour is systematically studied and is discussed in depth according to castor oil con-

centration and chemical potential inside and outside of the droplets.

2. Experimental

2.1. Materials

Monomers of methyl 2-methylprop-2-enoate (MMA) (99%; stabilised with 10–20 ppm MEHQ, Acros) and 2-ethylhexyl prop-2-enoate (EHP) (98%, Aldrich) were used as received. *tert*-butyl benzenecarboxperoxyate (Aldrich) was used as initiator for the radical polymerisation, triggered by the redox reaction with sodium ascorbate (Aldrich) or ascorbic acid (Aldrich). Castor oil (Fluka, 1000 mPas at 20 °C) was used to carry the active component, Polyphase P100 (3-iodoprop-2-yn-1-yl butylcarbamate (IPBC), Troy). Sodium dodecylsulphate (SDS) (>90%, Fluka) was used as emulsifier in stabilising the monomer emulsions. Toluene (+99%, Aldrich) was used as solvent in cleaning the disperse path in the membrane emulsification system. An industrial detergent of Decon 90 (5 wt% aqueous solution) was used to clean the continuous path.

2.2. Crossflow membrane emulsification (XME)

XME was used to manufacture the oil in water emulsions [19–21]. The technique uses a tubular ceramic membrane, which is fixed in a cylindrical stainless-steel shell module (Fig. 1). The disperse (oil) phase containing variable amounts of MMA, EHP, castor oil and IPBC is in the annulus to penetrate the membrane pores under a constant pressure of a pure nitrogen stream, and the aqueous (product) phase is recirculated via a pump (Jabsco 24 Series rotary lobe pump) crossflowing over the membrane surface. The droplets are then recirculated in the continuous phase until all the disperse phase is pushed through the membrane whereafter the product is bled-off.

Specially fabricated tubular ceramic membranes (\emptyset 20 \times 600 mm) (Mantec Filtration, UK) were used; each having 7 star-shaped parallel channels [22] with an effective inner diameter of 4 mm and with each ceramic tube having an internal surface area of $7.308 \times 10^{-2} \text{ m}^2$. The inner channel surfaces were slip-coated with finer alumina to reduce pore size, resulting in approx-

Table 1
Recipes used for preparing the emulsions.

Run number	Disperse phase						Aqueous phase				XME conditions		
	MMA (ml)	EHP (g)	Castor oil (ml) %		IPBC (g)	<i>tert</i> -butyl benzenecarboxperoxyate (g)	SDS (g)	Sodium ascorbate (g)	Sodium bicarbonate (g)	Ascorbic acid (g)	Duration (min)	Aqueous flow rate (ml/h)	Oil flux $\times 10^{-2}$ ($\text{m}^3/\text{m}^2 \text{ h}$)
1	0	0	370	100	0	0	1%	–	–	–	180	123	0.17
2	500	0	0	0	0	0	1%	–	–	–	9	> 3333	>4.56
3	0	420	0	0	0	0	1%	–	–	–	9	> 2800	>3.83
4	300	4.0	100	23.5	24.0	5.4	10.0	2.2	2.2	–	5	> 4800	6.57
5	300	4.0	100	23.5	24.4	5.5	10.0	–	–	2.2	5	4800	6.57
6	300	4.2	100	23.4	24.6	5.4	10.3	2.3	–	–	5	4800	6.57
7	300	4.1	100	23.2	24.9	10.8	10.3	4.4	–	–	5	4800	6.57
8	300	4.0	100	23.5	24.6	5.3	10.8	2.3	–	–	5	4800	6.57
9	300	4.1	25	7.1	24.8	5.4	10.0	0.7	–	–	5	4224	5.34
10	300	4.2	50	13.3	24.2	5.4	10.4	0.7	–	–	5	4200	5.75
11	300	4.0	100	23.5	24.3	5.4	10.3	0.7	–	–	5	4800	6.57
12	350	4.1	50	11.8	24.3	5.5	10.1	0.7	–	–	5	4800	6.57
13	362	4.1	38	9.0	24.3	5.3	10.7	0.7	–	–	5	4800	6.57
14	375	4.3	25	5.9	24.1	5.4	10.9	0.7	–	–	5	4800	6.57
15	384	4.1	13	3.1	24.3	5.3	10.3	0.7	–	–	5	4800	6.57
16	600	8.1	200	21.1	144.1	10.6	10.4	0.2	–	–	8	>6000	8.21
17	650	8.0	150	15.8	144.9	10.0	10.2	–	–	2.1	8	6000	8.21
18	700	8.0	100	10.6	143.7	10.0	10.8	–	–	2.1	8	6000	8.21
19	750	8.1	50	5.3	144.4	10.1	10.1	–	–	2.1	8	6000	8.21

Notes: Aqueous phase 1000 ml water; XME cross flow velocity 1.89 ms^{-1} except runs 1 and 3 when 1.93 ms^{-1} .

imately 0.2 μm pores with a span of approximately 0.3–0.8 [19] and a surface porosity of $\sim 10\%$.

Table 1 lists the recipes used for preparing the emulsions. Fresh tap water (Table S1) was used to prepare the aqueous phase (1000 ml of 1 wt% SDS for all runs). A transmembrane pressure of 0.3 MPa and a cross flow velocity of 1.89–1.93 m/s were used in the membrane emulsification at room temperature. The emulsions and the resulting samples were stored in the fridge before polymerisation for encapsulation.

2.3. Encapsulation

The standard method for the polymerisation was: charging approximately 20% of the monomer emulsion produced from the XME to a reactor (2 L) positioned within a water bath at 30 $^{\circ}\text{C}$, under a nitrogen blanket and stirred at 100 rpm. The monomer emulsion charge was initiated with approximately 20% of the ascorbic acid (or sodium ascorbate), as listed in Table 1, (dissolved in water), and then left to react for 1 h. The stirring speed was then increased to 200 rpm and the remainder of the monomer emulsion was fed into the reactor over a 2 h period. The initiator solution was also proportionally added. On completion of the feeds the reactant was left stirring for another 1 h. One run was carried out using a variation on the standard method (Run 6) (Table 1) used the water bath at 55 $^{\circ}\text{C}$. To check completion of polymerisation, a simple solids calculation was carried out by heating portions of samples at 150 $^{\circ}\text{C}$ for one hour. The results (Table S2) indicated that polymerisation was successfully completed.

2.4. Product characterisation

Size analyses of both the emulsion and microcapsule samples were performed using a Malvern Mastersizer 2000 (Malvern Instruments, in a Hydro S dispersion cell). Emulsion samples were dispersed in deionised water using a dispersion cell before being stirred and pumped at 1750 rpm through the measurement cell. The scattering pattern obtained is deconvoluted (to produce the particle size distribution) using Mie theory. The refractive index and absorption of the sample applied in these calculations are 1.49 and 0, respectively. The refractive index of the dispersant is taken as 1.33.

The amount of sample used was adjusted such that an obscuration of approximately 10% was obtained. Each sample was examined in three repeat measurement runs where each run consisted of ten separate measurements. Background and sample measurement times are 20 and 10 s, respectively. The average results of these multiple measurements are reported. The results are accurate up to $\pm 1\%$. For monomodal size distribution, the peak size and span, as defined by equation 1, are reported (in Table S2) for emulsion size and uniformity.

$$\text{Span} = (D_{90} - D_{10})/D_{50} \quad (1)$$

where D_{10} , D_{50} and D_{90} are the droplet size at the cumulated volume of the disperse phase at 10, 50 and 90 vol%, respectively.

The size retention % was determined by calculating the proportion of the emulsion droplets retaining their size after polymerisation.

3. Results and discussion

3.1. Emulsion size control by crossflow membrane emulsification

Membrane emulsification technology is robust in producing uniform size-predefined emulsion droplets from different disperse phases with very low to very high viscosity [6]. In crossflow mem-

brane emulsification (XME) the continuous phase is forced to flow across the membrane surface as shown in Fig. 1. A pressure is applied to the disperse phase which forces it to permeate the membrane pores and form disperse phase droplets on the inner surface of the membrane in the path of the flowing continuous phase. The shear force caused by the cross flowing assists in the detachment of the droplets formed into the continuous phase. It has been reported that emulsion droplets, in the range of 0.1–20 μm , produced using glass membranes have coefficient of variation (CV) values of 10% in connection with optimal formulation and operational conditions [6].

Initially emulsions were prepared of the individual components and a typical formulation prepared using them. Each component used (castor oil, MMA and EHP) was individually emulsified under the same conditions to examine their droplet formation in the membrane emulsification system (Table 1). (The size measurements are accurate up to $\pm 1\%$.) All three emulsions (Fig. 2a) had narrow monomodal size distributions with a peak at 0.9 μm and a span of 0.9 for the castor oil emulsion, a peak at 1.4 μm and a span of 0.8 for the MMA emulsion, and a peak at 4.7 μm and a span of 1.1 for the EHP emulsion (Table S2). These results are as expected for emulsion droplets which are produced one-at a time / individually from the membrane pores [24,25]. The ratios of droplet size to pore size found here (4.7 for castor oil, 6.9 for MMA and 23.6 for EHP) compare well with reported ratios in the range of 2 to more than 10 [6,22,23]. In addition, the flux for castor oil was lower than for MMA or EHP by a factor of ~ 20 (Table 1) which can be attributed to the difference in their viscosity (castor oil 650 mPa s compared with MMA 0.6 mPa s [17]).

After preparing emulsions of the individual components, an emulsion was prepared using a formulation typically used for encapsulation, using the same experimental conditions. The disperse phase contained 69.5 wt% of MMA, 1 wt% of EHP, 23.6 wt% of castor oil and 5.9 wt% of IPBC (Run 4). The freshly prepared emulsion had a narrow monomodal size distribution (Fig. 2b) with a peak at 2.8 μm and a span of 0.8 (Table S2). Both peak size and ratio of droplet size to pore size (14.1) are in-between the values for castor oil/MMA and EHP, indicating the large influence that EHP has even though it is present in only the small amount of 1 wt%.

After all the disperse phase had gone through the membrane in five minutes, the emulsion was further circulated in the rig at the same speed for 6 h to examine the droplet stability. The size analysis at each hour (Fig. 2b) is similar to other low viscous oil emulsions [26]. The emulsion experienced a size refining process, with the peak size shifting from 2.8 μm to 1.7 μm after one hour circulation, then gradually reducing to 1.4 μm after six hour circulation (Table S2). The circulation rate used (1.89 m/s) corresponds to a Reynold number (Re) of approximately 7600, which is well above the laminar flow range ($Re < 2300$) and in the turbulent flow range ($Re > 4000$) of a fully developed flow.

In summary, XME provides narrow monomodal sized emulsions which have sufficient stability for processing handling and for subsequent encapsulation.

3.2. Polymerization for encapsulation

The recipes used for preparing emulsions and microcapsules are listed in Table 1. The disperse phase contains MMA and EHP as monomers for the encapsulation, as well as castor oil and IPBC. 1.0 wt% of the EHP based on the disperse phase was kept constant in all the experiments to modify the brittle feature of PMMA. Castor oil has bifunction in the formula as the IPBC carrier (by dissolving it), and hydrophobe in maintaining the suspension polymerisation. The continuous phase contained 1 wt% of SDS, which corresponds to a molar concentration of 31.0 mM, which

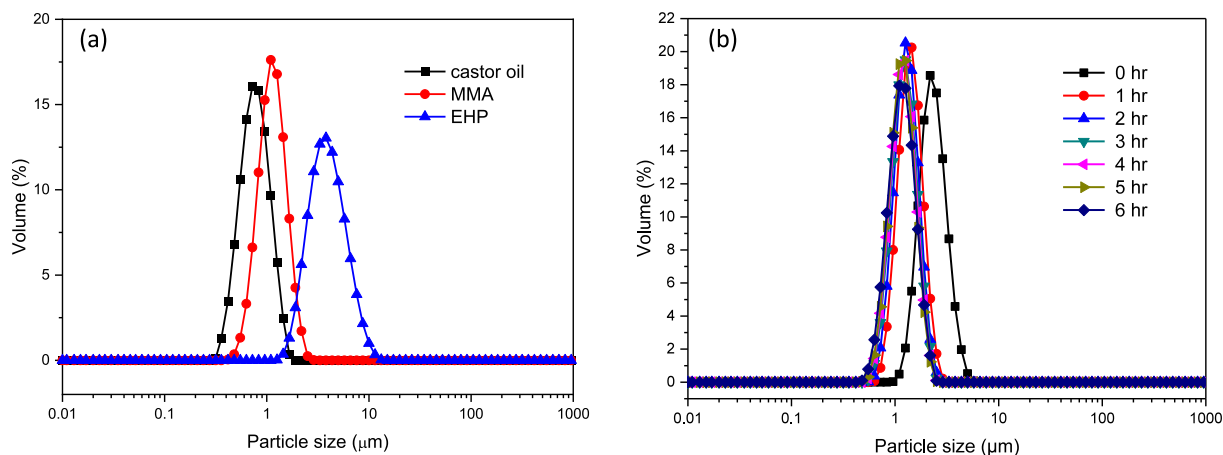


Fig. 2. Volume size distribution of emulsions of a) pure castor oil (1 h) (run 1), MMA (9 min) (run 2) and EHP (9 min) (run 3); b) a MMA solution (5 min) and as a function of time during emulsification of MMA formulation (run 4).

is well above the CMC of SDS in pure water (8.27 mM at 25 °C [11]). For each formulation, volume size distributions are shown in the [Supplementary Information](#), with representative/summary figures shown here. Table S2 has the data in a summary form.

3.2.1. Polymerisation of MMA emulsions

Initially, the manner of the polymerisation (emulsion or suspension) was investigated by making two formulations consisting of 1 wt% EHP, 6 wt% IPBC, radical initiator *tert*-butyl benzenecarboxyperoxy and significantly different proportions of castor oil: 5.8 wt% (Run 14) and 23.3 wt% (Run 11). Both emulsions were then heated to 30 °C with the addition of aqueous sodium ascorbate solution to trigger the radical initiator *tert*-butyl benzenecarboxyperoxy inside the droplets for the polymerisation. Fig. 3 shows the size distributions of these two emulsions and their polymerised particles. The emulsion containing 5.8 wt% castor oil (Fig. 3a) shows a narrow peak at 1.1 μm. After polymerisation, this peak almost disappeared. Nearly all the monomer in the precursor droplets escaped to the continuous phase, where they nucleated and formed particles at sizes of ~0.1 μm. This shows that the polymerisation was carried out in the manner of emulsion polymerisation rather than in-situ/suspension polymerisation. The inside out polymerisation provides little possibility to encapsulate the active component.

In contrast, the emulsion and polymerised particles from the formulation with 23.3 wt% of castor oil (Fig. 3b) have virtually the same size and size distribution with a peak size at 3.1 μm. Monomer escaping is suppressed in this case, instead suspension polymerisation is carried out encapsulating the active component. This agrees with Bux et al. [17] who used the same experimental set-up as we employed and found that the size distribution of MMA/castor oil microcapsules made with 12% and 24% castor oil closely matched that of the precursor monomer droplets indicating suspension polymerisation. The microcapsules made using 12% castor oil were examined by SEM and found to have essentially smooth surfaces. In addition TEM analyses were reported which confirmed the inclusion of the oil within the particles in a matrix-type structure. As we used the same experimental set-up a matrix-type structure is expected for the microcapsules reported here.

To examine the effect of the type (sodium ascorbate or ascorbic acid) and amount of the initiator trigger (0.7–4.4 g sodium ascorbate) on the polymerisation and encapsulation, the successful formula with ~23 wt% castor oil was used for a number of runs. For each run, the size distribution of the emulsion and its resulting

polymerised samples were similar (Runs 11, 5, 6, 7) ([supplementary information](#)) with narrow monomodal size emulsions, indicating that these variations did not alter suspension polymerisation from occurring.

When varying type of initiator trigger, for standard amount (Fig. 4a) there was a small difference in size distribution between sodium ascorbate (Run 11) (3.1 μm) and ascorbic acid (Run 5) (2.4 μm) (Table S2). When varying the quantity of the initiator trigger sodium ascorbate (Fig. 4b) there was a small difference in size distribution between lower (0.7 g) (Run 11) (3.1 μm), medium (2.3 g) (Run 6) (2.5 μm) and higher amounts (4.4 g) (Run 7) (2.7 μm) (Table S2) of sodium ascorbate.

As well as the standard temperature of 30 °C for the polymerisation (e.g. Run 11) a higher temperature of 55 °C was also examined. The size distributions of the precursor emulsion and polymerised microcapsules (Run 8, [Supplementary Information](#)) reveal that microcapsules formed at 55 °C have a similar size distribution pattern to the emulsion droplets, but with a significantly larger average size (emulsion 2.0 μm; microcapsules 2.3 μm). This is different from the emulsion polymerised at 30 °C (eg Fig. 3b, Table S2) which copied the droplet size distribution. It is known that the densities of oils decrease upon increasing temperature [27]. So the larger particles obtained at 55 °C may have arisen through the droplets swelling at the increased temperature before polymerisation occurring and forming a solid structure. This suggests that in other runs slight variation in the temperature used in the polymerisation step could be a source of slight variation in size.

The effect of polymerisation time on the encapsulation was examined by increasing the reaction time from 1 h to 48 h after the polymerisation was initiated (Run 6) ([Supplementary Information](#)). The size examination showed little difference: 2.51 μm (24 h), 2.50 μm (41 h), 2.48 μm (48 h).

In summary, both sodium ascorbate and ascorbic acid work similarly as an initiator trigger to trigger the radical initiator inside the emulsion droplets for the suspension polymerisation. Consequently, for studying the effect of castor oil, both sodium ascorbate and ascorbic acid were used to prepare emulsions whilst a standard temperature of 30 °C was used in the polymerisations with a reaction time of 1 h.

3.2.2. Effect of castor oil

To examine the effect of castor oil in the encapsulation mechanism, three series of runs were prepared using variable amounts of monomer mixtures. Series A used a fixed amount of MMA and a

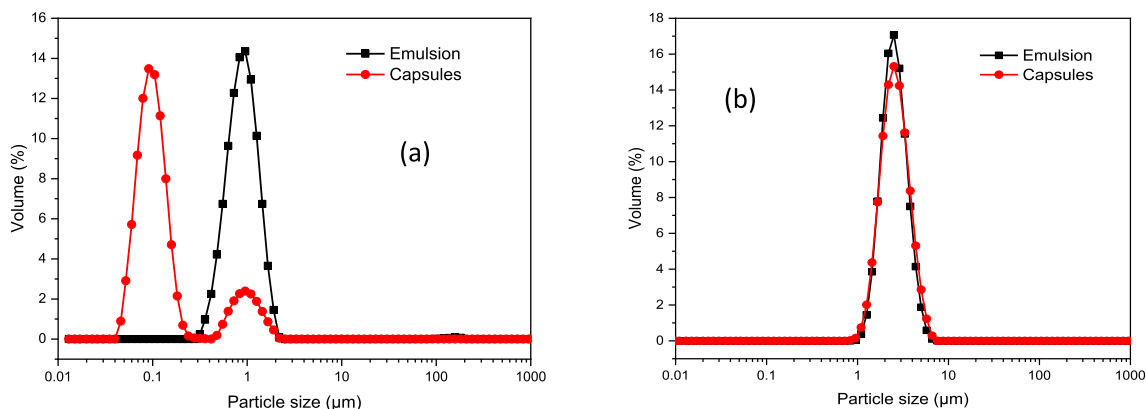


Fig. 3. Volume size distribution of prepared emulsions and polymerised samples of two formulations consisting of significantly different proportions of castor oil: a) 5.8% (run 14) and b) 23.3% (run 11).

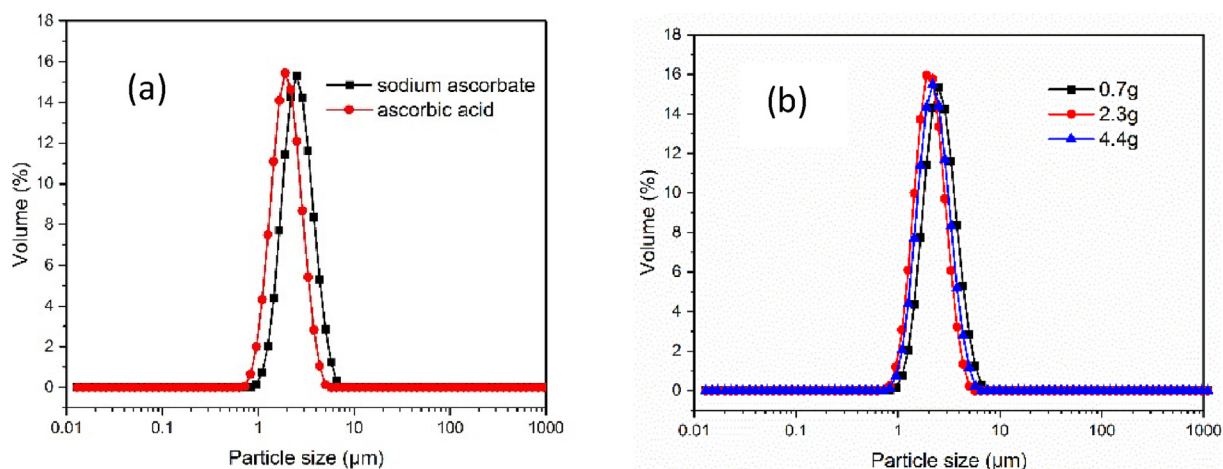


Fig. 4. Volume size distribution of polymerised samples a) with varying type of initiator (sodium ascorbate (run 11) and ascorbic acid (run 5), b) with variable amounts of initiator trigger (sodium ascorbate) (runs 11/6/7).

variable amount of castor oil; Series B used a fixed combined volume of (MMA and castor oil) with a variable ratio; Series C was similar to Series B except that the volume of monomer mixtures used was double, and the amount of active ingredient was higher.

Series A used a fixed amount of MMA (300 ml), a variable amount of castor oil decreasing from 23.5 wt% (which Run 11 has shown to enable suspension polymerisation) to 7.1 wt% and a fixed amount of IPBC of 6 wt%. The mixture generated emulsions with a volume concentration of approximately 40% v/v. The emulsions prepared all had similar narrow monomodal size distributions (Fig. 5a) with peak sizes in the range of 1.9–3.1 μm (Table S2), increasing in size with castor oil content. The polymerised particles (Fig. 5b) have virtually the same size and size distribution as their respective emulsions (Table S2).

Series B used a fixed total volume of (MMA and castor oil) (400 ml) and varied the individual ratios used, with the amount of castor oil varying from 23.5 to 3.1 wt%, with a fixed IPBC content of approximately 6 wt% and a volume concentration of approximately 40% v/v. The emulsions prepared using 23.5 to 5.9 wt% castor oil all had narrow monomodal size distributions with peak sizes in the range of 1.1–3.1 μm (Table S2), whilst the emulsion prepared with 3.1 wt% had a bimodal peak (Fig. 5c) with peaks at $\sim 1 \mu\text{m}$ and $\sim 200 \mu\text{m}$ (Table S2). The peak at $\sim 1 \mu\text{m}$ fits in with the pattern of lowering peak size with decreasing castor oil %. Consequently, the peak at $\sim 200 \mu\text{m}$ may have arisen through agglomeration of the smaller sized droplets.

After polymerisation, the run with 23.5 wt% of castor oil replicated the monomodal size distribution of its emulsion precursors (Fig. 5d). The run with 11.8 wt% castor oil showed bimodal size distribution with peaks at 0.1 and 2.1 μm (Table S2). The runs with less than 9 wt% castor oil formed their major volume peaks at 0.1 μm and a smaller peak in the size range of their precursor emulsion. This peak decreases as the amount of castor oil decreases. The presence of two peaks upon castor oil reduction together with one of them being at 0.1 μm suggests the two polymerisation mechanisms are occurring simultaneously.

Series C was similar to Series B except that the volume of monomer mixtures used was double (800 ml) with the amount of castor oil varying from 21.1 to 5.3 wt% with the amount of IPBC increased to 15.9 wt% and a volume emulsion concentration of approximately 80% v/v. All the emulsions produced showed narrow monomodal size-distributions (Fig. 5e) with peak sizes in the range of 1.4–2.8 μm (Table S2). Again, the higher the castor oil content the larger the droplets formed. Fig. 5f shows their particle size analysis after polymerisation. The runs with 21.1 to 10.6 wt% of castor oil demonstrated replicated particle size distribution with peak sizes of 1.9–2.7 μm (Table S2), while the formulation with 5.3 wt% of castor oil showed a dominant peak at $\sim 0.1 \mu\text{m}$ and a small peak in the size range of its emulsion. It was observed that all of Series C had fouling, eg formation of lumps, with the amount increasing with castor oil. As most of the runs had monomodal size distributions (Runs 16, 17, 18) this suggests the fouling was due to

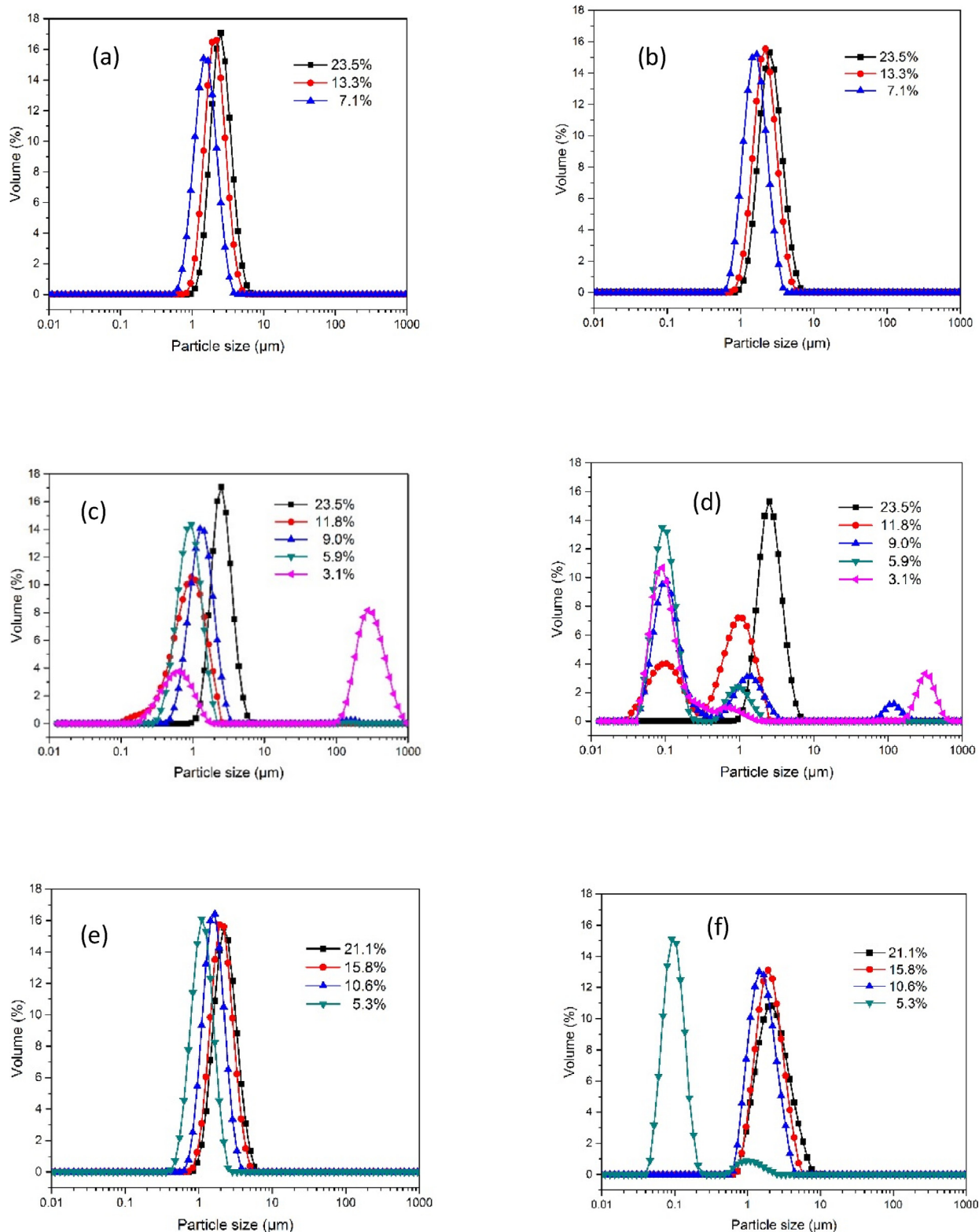


Fig. 5. Volume size distribution of a) prepared emulsions and b) polymerised sample (Series A runs 9–11); c) prepared emulsions and d) polymerised sample) (Series B runs 11–15); and e) prepared emulsions and f) polymerised sample (Series C runs 16–19) where Series A contains 300 ml MMA and variable % castor oil (runs 9–11), Series B fixes the combined volume of MMA and castor oil (400 ml) (runs 11–15) and Series C fixes the combined volume of MMA and castor oil (800 ml) (runs 16–19).

polymerised capsules sticking together. Such coalescence/flocculation might be encouraged by the higher level of emulsion concentration in Series C (80% v/v) compared with Series A and B (40% v/v) and suggests that there is an upper limit to stable emulsion concentration.

Discussion Comparing the results for Series A (Fig. 5b), B (Fig. 5d), and C (Fig. 5f) it can be seen that the concentration of the castor oil in the disperse phase plays a crucial role in determining the polymerisation mechanism. The encapsulated proportion of Series A, B and C versus castor oil concentration is plotted in Fig. 6,

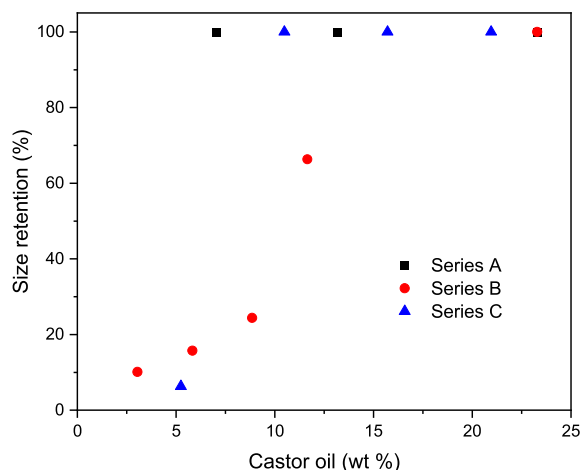


Fig. 6. Effect of castor oil concentration on size retention % (where size retention refers to the proportion of emulsion droplets retaining their size on polymerization) (Series A (runs 9–11), Series B (runs 11–15) and Series C (runs 16–19)).

where with low levels of castor oil the polymerisation was carried out in the manner of emulsion polymerisation, and with high levels of castor oil, suspension polymerisation was enabled, which agrees with Fig. 3. This is in agreement with Bux et al. [17] who found that the size distribution of MMA/castor oil microcapsules made with 12% and 24% castor oil closely matched the precursor monomer droplets indicating suspension polymerisation, and also Steinmacher et al. [16] who used 50 wt% of castor oil in MMA and obtained suspension polymerisation. However, the experimental results (Fig. 6) show a mixed emulsion and suspension polymerisation in the range of 6–12 wt%. The amount of castor oil alone in this range cannot be used to accurately predict the polymerisation mechanism. This suggests the involvement of an additional factor.

Another aspect is the variation in the size of the transition concentration between the different Series. It is unclear why there is some variation between Series A and B when they have similar emulsion concentrations (40%). However, the differences between Series B and C may be due to Series C having a higher level of emulsion (80%) compared with Series B (40%).

It has been demonstrated that the stability of a miniemulsion is proportional to the molar concentration of the osmotic agent (hydrophobe) in the dispersed phase [15]. *n*-hexadecane has typically been used in literature emulsion systems [28] usually in the concentration 4 wt% or 0.169 mmol g⁻¹ of the dispersed phase [15]. Barrios et al. [15] investigated the use of hydrocarbon coumarone-indene resins resin (HCR) as an osmotic agent. They found that 0–6.5 wt% HCR were not able to stabilise the miniemulsion but 9 and 12 wt% did. Using the molecular weight (Mn) of HCR (~590 g mol⁻¹), the equivalent weight concentration of HCR (0.169 mmol g⁻¹) was calculated as 10.4 wt% of the dispersed phase which fits with the results.

For castor oil (molecular weight ~928 g mol⁻¹) [29], the equivalent weight concentration of castor oil (0.169 mmol g⁻¹) is 16.5 wt%. This is significantly more than the 8–12 wt% observed (Fig. 6). This difference may be accounted for by the presence of the IPBC component (usually ~6 wt%) also playing the role of a hydrophobe as the use of a biocide (SeaNine211) as a hydrophobe in a miniemulsion MMA based polymerization has been observed before [30]. An additional factor is that whilst some hydrophobes e.g. hexadecane are aliphatic, castor oil contains ricinoleic acid which has C=C double bonds [16]. These can undergo copolymerisation with MMA, resulting in castor oil being less available to act as a hydrophobe. Using the experimental results, the influence of the biocide IPBC and other components in both the disperse phase

and continuous phase are investigated based on changes in chemical potential.

3.3. Discussion on formulation and encapsulation around the chemical potential balance

It has been believed [6,19,26] that Laplace pressure provides the driving force for the diffusion of disperse molecules to the continuous phase, and the higher Laplace pressure in small droplets drives the molecules to diffuse to larger droplets via the continuous phase for Oswald ripening. However, Laplace pressure, caused by curvature, technically would not be related to molecule diffusion, as McClements et al. observed through a droplet solubility study of an O/W emulsion [31–33]. McClements et al. first prepared stock O/W emulsions (~300 nm) in the presence of aqueous surfactant micelles. The stock emulsions were then diluted using pure water or the surfactant solution (>CMC). The droplet population and size analysis with time showed that pure water dilution did not result in significant changes. In contrast, the dilution with the surfactant solution resulted in decreased droplet population and increased droplet sizes. The larger the solubility of the oil in water, the more significant the change was. These results show that Oswald ripening is not only to do with droplet sizes, but also closely connected with the surfactant concentration in the continuous phase. If we take the surfactant stabilised oil/water interface as a semi-permeable membrane, there would be osmotic pressure on both sides (Fig. S1). The osmotic pressures inside (π_{in}) and outside (π_{out}) the droplet, in relation to monomer and water, respectively, would be responsible for the molecule diffusion, similar to the stabilisation issues in a double emulsion [34]. However, this theory saw an overlap range where the relative osmotic pressure cannot distinguish the one-to-one copied encapsulation in the failed ones. Consequently, we examined the effect of chemical potential difference between inside and outside of the droplet.

The chemical potentials of monomer and water depend on their concentration in their corresponding phases, which can be expressed as:

$$\mu_{mono}^{in}(T, P, \chi_{mono}) = \mu_{mono}^*(T, P) + RT \ln \chi_{mono} \quad (2)$$

$$\mu_{water}^{out}(T, P, \chi_{water}) = \mu_{water}^*(T, P) + RT \ln \chi_{water} \quad (3)$$

where $\mu_{mono}^{in}(T, P, \chi_{mono})$ is the chemical potential of the monomer inside the droplet at temperature *T*, pressure *P* and molar fraction of the monomer in the disperse phase χ_{mono} ; $\mu_{water}^{out}(T, P, \chi_{water})$ is the chemical potential of water in the continuous phase at temperature *T*, pressure *P* and molar fraction of the water in the continuous phase χ_{water} ; $\mu_{mono}^*(T, P)$ and $\mu_{water}^*(T, P)$ refer to the chemical potentials of the pure monomer and water at *T* and *P*, respectively.

The chemical potential difference between the inside and outside of the droplet can then be obtained by subtracting Equation (3) from 2, resulting in Equation (4) where the chemical potential difference is related to the molar fraction ratio of monomer and water (the volatile components) in their own phases.

$$\begin{aligned} \mu_{mono}^{in}(T, P, \chi_{mono}) - \mu_{water}^{out}(T, P, \chi_{water}) \\ = constant + RT \ln \chi_{mono} / \chi_{water} \end{aligned} \quad (4)$$

$$constant = \mu_{mono}^*(T, P) - \mu_{water}^*(T, P)$$

Equation (4) suggests that the chemical potential difference between the monomer inside and water outside of the droplet can be adjusted by varying their molar fraction ratio. For a positive chemical potential difference, the monomer inside the droplet has a higher chemical potential tending to diffuse out. For a negative value, the water outside the droplet has a higher chemical potential. In this case, water tends to diffuse into the droplet, while for

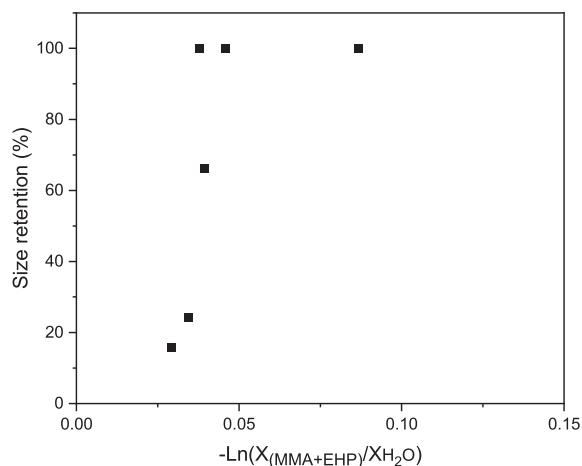


Fig. 7. Relationship between the size retention % and the molar fraction ratio of the monomer (MMA + EHP) components within droplet to that of water the continuous phase. (Castor oil in the range of 5.8–13.2% (runs 14, 9, 13, 18, 12, 10)).

the value of zero the chemical potential of the monomer inside the droplet equals that of the water outside of the droplet. In this case, for both the monomer and water the net diffusion is zero across the droplet surface membrane, and so the one-to-one copied encapsulation occurs.

The relationship between the size retention % against $-\ln\chi_{\text{mono}}/\chi_{\text{water}}$, where the monomer is the sum of MMA and EHP (combined due to their close properties and the small amount of EHP present ($\sim 1\%$ (v/v) of MMA), in the transition range of 6–12 wt% castor oil is shown in Fig. 7. It shows that the size retention % increases with $-\ln\chi_{\text{mono}}/\chi_{\text{water}}$ from below 20% to 100% with a sharp transition of $-\ln\chi_{\text{mono}}/\chi_{\text{water}}$ value at ~ 0.046 as it goes from partial to full encapsulation. When $-\ln\chi_{\text{mono}}/\chi_{\text{water}}$ is > 0.046 , one to one copied (100%) encapsulation is achieved, while when $-\ln\chi_{\text{mono}}/\chi_{\text{water}}$ is smaller than 0.046 the encapsulation rate decreases drastically.

Putting this data back into Equation (4), one can interpret that the $\text{constant} = \mu_{\text{mono}}^*(T, P) - \mu_{\text{water}}^*(T, P)$ gives a positive value. As $-\ln\chi_{\text{mono}}/\chi_{\text{water}}$ increases, the chemical potential difference between the monomer inside and water outside the droplet ($\mu_{\text{mono}}^{\text{in}}(T, P, \chi_{\text{mono}}) - \mu_{\text{water}}^{\text{out}}(T, P, \chi_{\text{water}})$) decreases and reaches zero at $-\ln\chi_{\text{mono}}/\chi_{\text{water}} = 0.046$. The 0.046 value is critical and corresponds to a chemical potential of $0.046RT$ (116 J/mol at 30 °C), which is equal to $\mu_{\text{mono}}^*(T, P) - \mu_{\text{water}}^*(T, P)$. This chemical potential difference can be taken as an energy barrier that is required to avoid monomer diffusing across the membrane in the system. This value is significantly less than that of hydrogen bonds in bulk water (10.6 kJ/mol) [35] suggesting that the energy barrier for the monomer molecules to escape is very low. The energy barrier of ≥ 116 J/mol represents an essential requirement for formulating a complex emulsion system that is stable enough for encapsulation processing by suspension polymerisation.

4. Conclusion

Emulsification-polymerisation is one of the most attractive methods for the production of microcapsules with active components for controlled delivery. However, monomers in emulsion droplets tend to escape out into the aqueous continuous phase during the polymerisation for encapsulation. This is only partially understood and summarised as 1) introducing a hydrophobe with a minimum concentration in the monomer droplet [8,9] such as

hexadecane which is typically used [15] and 2) depleting free micelles of surfactant in the aqueous continuous phase [10] to avoid the escape of monomer.

The experimental results show that castor oil can successfully act as a hydrophobe for the encapsulation of an active component (6.0–15.9 wt% IPBC in poly(methyl 2-methylprop-2-enoate)) in the presence of a large amount of free surfactant micelles. The concentration of castor oil in the disperse phase plays an important role: > 12 wt% gives rise to full encapsulation (which agrees with previous results for 12–50% [16,17]), whilst < 6 wt% results in only a small portion of particles remaining in the emulsion size range, indicating a lack of encapsulation. However, when the castor oil concentration is in the range of 6–12 wt% either full or partial encapsulation is obtained, which cannot be explained by any existing theory.

The > 12 wt% of castor oil required is less than the 16.5 wt% of hexadecane that would be required to fit the normal molar amount suggested [15] and raises the possibility of the IPBC playing the role of a hydrophobe (cf SeaNine211 [30]).

In this work the chemical potential difference between inside and outside the droplets was studied to comprehend the influence of IPBC, surfactant and other existing components that contribute to the colligative properties of the two phases in the system. The study shows that a critical molar fraction ratio of the monomer (MMA with a small amount of EHP) in the droplet to that of the water in the continuous phase exists for successful encapsulation. This critical ratio corresponds to an energy barrier of 116 J/mol that exists to prevent the monomer components escaping from the droplets in the system studied. This value is significantly less than that of hydrogen bonds in bulk water (10.6 kJ/mol) [35] suggesting that the energy barrier for the monomer molecules to escape is in the lower end of secondary forces involved.

Future work will determine the energy barrier using different monomers and hydrophobes to determine if the energy barrier is independent or related to the nature of the monomer and/or hydrophobe used.

Declaration of Competing Interest

The authors declare that they have no known competing financial interests or personal relationships that could have appeared to influence the work reported in this paper.

Acknowledgement

We are grateful to ICI (now AkzoNobel) for a grant (SRF2516) to carry out this work and for permission to publish this paper.

Appendix A. Supplementary material

Supplementary data to this article can be found online at <https://doi.org/10.1016/j.jcis.2022.05.014>.

References

- [1] D.R. Perinelli, G.F. Palmieri, M. Cespi, G. Bonacucina, Encapsulation of Flavours and Fragrances into Polymeric Capsules and Cyclodextrins Inclusion Complexes: An Update, *Molecules* 25 (2020) 5878, <https://doi.org/10.3390/molecules25245878>.
- [2] S. Praveen, D.J. He, Microencapsulation of vitamins in food applications to prevent losses in processing and storage: A review, *Food Res. Int.* 137 (2020), <https://doi.org/10.1016/j.foodres.2020.109326> 109326.
- [3] I.T. Carvalho, B.N. Estevinho, L. Santos, Application of microencapsulated essential oils in cosmetic and personal healthcare products – a review, *Int. J. Cosmet. Sci.* 38 (2016) 109–119, <https://doi.org/10.1111/ics.12232>.
- [4] B.B. Huang, S.F. Zhang, P.H. Chen, G. Wu, Release and Degradation of Microencapsulated Spinosad and Emamectin Benzoate, *Sci. Rep.* 7 (2017) 10864, <https://doi.org/10.1038/s41598-017-11419-2>.

- [5] S. Higashi, T. Setoguchi, Hepatic arterial injection chemotherapy for hepatocellular carcinoma with epirubicin aqueous solution as numerous vesicles in iodinated poppy-seed oil microdroplets: clinical application of water-in-oil-in-water emulsion prepared using a membrane emulsification technique, *Adv. Drug Deliv. Rev.* 45 (2000) 57–64, [https://doi.org/10.1016/S0169-409X\(00\)00100-9](https://doi.org/10.1016/S0169-409X(00)00100-9).
- [6] R. Williams, Q. Yuan, S. Collins, Membrane Emulsification, *Encyclopedia of Surface and Colloid Science: Second Edition* (2010), <https://doi.org/10.1081/E-ECS-120045996>.
- [7] J. Bibette, D.C. Morse, T.A. Witten, D.A. Weitz, Stability Criteria for Emulsions, *Phys. Rev. Lett.* 69 (1992) 2439–2442, <https://doi.org/10.1103/PhysRevLett.69.2439>.
- [8] K. Landfester, N. Bechthold, F. Tiarks, M. Antonietti, Formulation and Stability Mechanisms of Polymerizable Miniemulsions, *Macromolecules* 32 (1999) 5222–5228, <https://doi.org/10.1021/ma990299+>.
- [9] L.L. Hecht, C. Wagner, K. Landfester, H.P. Schuchmann, Surfactant Concentration Regime in Miniemulsion Polymerization for the Formation of MMA Nanodroplets by High-Pressure Homogenization, *Langmuir* 27 (2011) 2279–2285, <https://doi.org/10.1021/la104480s>.
- [10] G. Ma, J. Li, Compromise between dominant polymerization mechanisms in preparation of polymer microspheres, *Chem. Eng. Sci.* 59 (2004) 1711–1721, <https://doi.org/10.1016/j.ces.2004.01.027>.
- [11] E. Matijević, B.A. Pethica, The heats of micelle formation of sodium dodecyl sulphate, *Trans. Faraday Soc.* 54 (1958) 587–592, <https://doi.org/10.1039/TF9585400587>.
- [12] B. Binks, *Modern Aspects of Emulsion Science*, The Royal Society of Chemistry, Cambridge, 1998, pp. 33–38. <https://doi.org/10.1039/9781847551474>.
- [13] R.J. Hunter, *Foundations of Colloid Science*, second ed., Oxford University Press, Oxford, 2000.
- [14] C.S. Chern, T. Chen, Miniemulsion polymerization of styrene using alkyl methacrylates as the reactive cosurfactant, *J. Colloid Polym. Sci.* 275 (1997) 546–554, <https://doi.org/10.1007/s003960050117>.
- [15] S.B. Barrios, J.F. Petry, C.K. Weiss, C.L. Petzhold, K. Landfester, Polymeric Coatings Based on Acrylic Resin Latexes from Miniemulsion Polymerization Using Hydrocarbon Resins as Osmotic Agents, *J. Appl. Poly. Sci.* 131 (15) (2014) n/a–n/a.
- [16] F.R. Steinmacher, N. Bernardy, J.B. Moretto, E.I. Barcelos, P.H.H. Araujo, C. Sayer, Kinetics of MMA and VAc Miniemulsion Polymerizations Using Miglyol and Castor Oil as Hydrophobe and Liquid Core, *Chem. Eng. Technol.* 33 (2010) 1877–1887, <https://doi.org/10.1002/ceat.201000256>.
- [17] J. Bux, M.S. Manga, T.N. Hunter, S. Biggs, Manufacture of poly(methyl methacrylate) microspheres using membrane emulsification, *Phil. Trans. R. Soc. A* 374 (2016) 20150134, <https://doi.org/10.1098/rsta.2015.0134>.
- [18] A. Nazira, G.T. Vladislavjević, Droplet breakup mechanisms in premix membrane emulsification and related microfluidic channels, *Adv. Colloid Interface Sci.* 290 (2021), <https://doi.org/10.1016/j.cis.2021.102393>.
- [19] R.A. Williams, S.J. Peng, D.A. Wheeler, N.C. Morley, D. Taylor, M. Whalley, D.W. Houldsworth, Controlled production of emulsions using a crossflow membrane. Part II. Industrial scale manufacture, *Trans. IChemE* 76 (1998) 902–910, <https://doi.org/10.1205/026387698525702>.
- [20] Q. Yuan, O.J. Cayre, M. Manga, R.A. Williams, S. Biggs, Preparation of Nanoparticle Stabilised Emulsions Using Membrane Emulsification, *Soft Matter* 6 (2010) 1580–1586, <https://doi.org/10.1039/B921372D>.
- [21] S. Collins, D.W. York, S. Kazmi, A.K. Mohammed, Formation of wax walled microcapsules via double emulsion using cross membrane emulsification at elevated temperatures, *J. Food Eng.* 269 (2020), <https://doi.org/10.1016/j.jfoodeng.2019.109739>.
- [22] F. Spyropoulos, D.M. Lloyd, R.D. Hancock, A.K. Pawlik, Advances in membrane emulsification. Part A: recent developments in processing aspects and microstructural design approaches, *J. Sci. Food Agric.* 94 (2014) 613–627, <https://doi.org/10.1002/jsfa.6444>.
- [23] S.M. Joscelyne, G. Trägårdh, Membrane emulsification—a literature review, *J. Membr. Sci.* 169 (2000) 107–117, [https://doi.org/10.1016/S0376-7388\(99\)00334-8](https://doi.org/10.1016/S0376-7388(99)00334-8).
- [24] S.J. Peng, R.A. Williams, Controlled Production of Emulsions Using a Crossflow Membrane, *Chem. Eng. Res. Des.* 76 (8) (1998) 894–901.
- [25] F. Spyropoulos, R.D. Hancock, I.T. Norton, Food-grade emulsions prepared by membrane emulsification, *Procedia Food Sci.* 1 (2011) 920–926, <https://doi.org/10.1016/j.profoo.2011.09.139>.
- [26] Q. Yuan, R.A. Williams, S. Biggs, Surfactant Selection for Accurate Size Control of Microcapsules Using Membrane Emulsification, *Colloids and Surf. A. Physicochem. Eng. Aspects* 347 (1–3) (2009) 97–103.
- [27] N.G. Porter, J.P. Lammerink, Effect of Temperature on the Relative Densities of Essential Oils and Water, *J. Essent. Oil Res.* 6 (1994) 269–277, <https://doi.org/10.1080/10412905.1994.9698375>.
- [28] J. Jeng, C.-A. Dai, W.-Y. Chiu, C.-S. Chern, K.-F. Lin, P.-Y. Young, Influence of Hexadecane on the Formation of Droplets and Growth of Particles for Methyl Methacrylate Miniemulsion Polymerization, *Journal of Polymer Science: Part A, Polym. Chem.* 44 (2006) 4603–4610, <https://doi.org/10.1002/pola.21534>.
- [29] N.L. Da Silva, C. Batistella, R. Maciel Filho, M.R. Wolf Maciel, Determination of Castor Oil Molecular Weight by Vapour Pressure Osmometry Technique, *Chem. Eng. Trans.* 24 (2011) 601–606, <https://doi.org/10.3303/CET1124101>.
- [30] M. Zhang, E. Cabane, J. Claverie, Transparent antifouling coatings via nanoencapsulation of a biocide, *J. Appl. Polym. Sci.* 105 (2007) 3826–3833, <https://doi.org/10.1002/app.26659>.
- [31] D.J. McClements, S.R. Dungan, Light scattering study of solubilization of emulsion droplets by non-ionic surfactants, *Colloids Surf A. Physicochem. Eng. Aspects* 104 (1995) 127–135, [https://doi.org/10.1016/0927-7757\(95\)03261-4](https://doi.org/10.1016/0927-7757(95)03261-4).
- [32] J. Weiss, J.N. Coupland, D.J. McClements, Solubilization of hydrocarbon droplets suspended in a non-ionic surfactant solution, *J. Phys. Chem.* 100 (1996) 1066–1071, <https://doi.org/10.1021/jp9524892>.
- [33] J. Weiss, J.N. Coupland, D. Brathwaite, D.J. McClements, Influence of molecular structure of hydrocarbon emulsion droplets on their solubilization in nonionic surfactant micelles, *Colloids Surf A. Physicochem. Eng. Aspects* 121 (1997) 53–60, [https://doi.org/10.1016/S0927-7757\(96\)03742-9](https://doi.org/10.1016/S0927-7757(96)03742-9).
- [34] A. Aserin, *Multiple emulsions: technology and applications*, Wiley-Interscience, 2008.
- [35] D. van der Spoel, P.J. van Maaren, P. Larsson, N. Timneanu, Thermodynamics of hydrogen bonding in hydrophilic and hydrophobic media, *J. Phys. Chem. B* 110 (2006) 4393–4398, <https://doi.org/10.1021/jp0572535>.